SCIENTIFIC REPORTS

OPEN

SUBJECT AREAS:
ELECTRONIC DEVICES
CARBON NANOTUBES AND FULLERENES
MOLECULAR ELECTRONICS

Received
16 October 2014

Accepted
22 December 2014

Published
22 January 2015

Correspondence and requests for materials should be addressed to T.F. (fujigaya-tcm@mail.cstm.kyushu-u.ac.jp) or N.N. (nakashima-tcm@mail.cstm.kyushu-u.ac.jp)

Development of n-type cobaltocene-encapsulated carbon nanotubes with remarkable thermoelectric property

Takahiro Fukumaru[1], Tsuyohiko Fujigaya[1,2] & Naotoshi Nakashima[1,2,3]

[1]Department of Applied Chemistry, Graduate School of Engineering, Kyushu University, 744 Motooka Nishi-ku, Fukuoka 819-0395, Japan, [2]International Institute for Carbon-Neutral Energy Research (WPI-I2CNER), Kyushu University 744 Motooka Nishi-ku, Fukuoka 819-0395, Japan, [3]JST-CREST, 5 Sanbancho, Chiyoda-ku, Tokyo, 102-0075, Japan.

Direct conversion from heat to electricity is one of the important technologies for a sustainable society since large quantities of energy are wasted as heat. We report the development of a single-walled carbon nanotube (SWNT)-based high conversion efficiency, air-stable and flexible thermoelectric material. We prepared cobaltocene-encapsulated SWNTs (denoted $CoCp_2$@SWNTs) and revealed that the material showed a negative-type (n-type) semiconducting behaviour (Seebeck coefficient: $-41.8\ \mu V\ K^{-1}$ at 320 K). The $CoCp_2$@SWNT film was found to show a high electrical conductivity (43,200 $S\ m^{-1}$ at 320 K) and large power factor (75.4 $\mu W\ m^{-1}\ K^{-2}$) and the performance was remarkably stable under atmospheric conditions over a wide range of temperatures. The thermoelectric figure of merit (*ZT*) value of the $CoCp_2$@SWNT film (0.157 at 320 K) was highest among the reported n-type organic thermoelectric materials due to the large power factor and low thermal conductivity (0.15 $W\ m^{-1}\ K^{-1}$). These characteristics of the n-type $CoCp_2$@SWNTs allowed us to fabricate a p-n type thermoelectric device by combination with an empty SWNT-based p-type film. The fabricated device exhibited a highly efficient power generation close to the calculated values even without any air-protective coating due to the high stability of the SWNT-based materials under atmospheric conditions.

Thermoelectric conversion is one of the key technologies to realize a sustainable society since large quantities of energy (roughly 15 terawatts per year)[1] have been wasted as heat[2]. A number of semiconducting materials including inorganic[3,4] and organic materials[5–7] function as thermoelectric materials that directly convert heat into electricity via a carrier movement in the materials based on the Seebeck effect. Especially, inorganic materials, such as Bi_2Te_3, Si/Ge and PbTe, have been intensively studied due to their high power factors that originated from the large Seebeck coefficients ranging from 100–45,000 $\mu V\ K^{-1}$[3,4] and high carrier conductivity. Recently, efficient harvesting of waste heat in a low temperature range (300–400 K) has attracted significant attention due to ready availability of such heat sources in daily life. In particular, cost, flexibility and mechanical toughness of energy harvesting materials are important[8,9].

Polymeric materials[5–9] including carbon nanotubes[10–13] have attracted much attention as substitutes in this temperature range due to their low cost, ease of fabrication, flexibility and light weight, despite their relatively low Seebeck coefficients (typically on the order of 5–200 $\mu V\ K^{-1}$). Very recently, Maniwa et al. reported that a sorted semiconducting single-walled carbon nanotube (SWNT) film shows a very large Seebeck coefficient (170 $\mu V\ K^{-1}$ at 300 K)[14]. Their report gave us a hint to design and develop an SWNT-based thermoelectric material with high performance. While SWNTs and conducting polymers are promising p-type organic thermoelectric materials as described above, the development of flexible n-type thermoelectric materials is still challenging even though at present, their thermoelectric performances are still low (the highest thermoelectric figure of merit is 0.2 at 440 K)[15] and they have low stability in air after doping[16]. Because n-type semiconducting organic materials are inherently unstable in air due to their oxidation, the key issue in order to develop a highly efficient thermoelectric device using a polymer is to evaluate an n-type material with a high stability, leading to the fabrication of a p-n connected thermoelectric device with a large power factor.

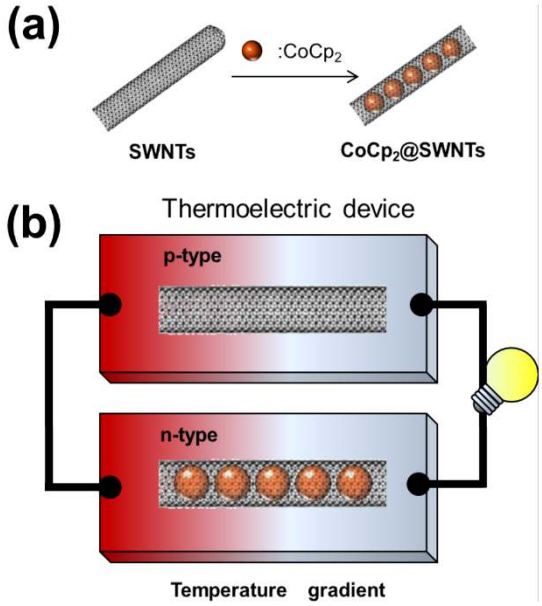

Figure 1 | Encapsulation of $CoCp_2$ into the SWNTs and the thermoelectric device composed of the SWNTs and $CoCp_2$-encapsulated SWNTs. (a,b) Schematic drawing of (a) an encapsulation of $CoCp_2$ into the SWNTs and of (b) a thermoelectric device composed of empty-SWNT and $CoCp_2$-encapsulated SWNT developed in this study.

In this study, we focused on the use of SWNTs as the polymeric materials since we can tune the electric property to either p- or n-type by chemical doping[17]. In addition, the flexibility of the film, mechanical toughness, high thermal stability and extremely high charge transport are quite attractive when considering the fabrication of environment-conscious devices. In order to tune the SWNTs to the n-type, doping of an alkali metal[18], viologen[19], hydrazine[20], coenzyme[21], 1*H*-benzoimidazole derivatives[22], polyethyleneimine (PEI)[23,24] and phosphorus compounds[8], as well as the doping of nitrogen into the SWNT bond[25], have been reported. In this study, we chose cobaltocene ($CoCp_2$) as the dopant for the encapsulation due to its strong reducibility (Fig. 1a)[26,27]. Among the variety of doping approach, we focused on encapsulation of the dopant molecules inside the SWNTs[26], which show a superior doping stability due to the molecular shielding effect compared to the doping on the outside the tubes[17]. Then, the SWNTs encapsulated with $CoCp_2$ ($CoCp_2$@SWNTs) were used to fabricate a p-n connected thermoelectric device without any air protective coating (Fig. 1b). This is the first report using encapsulated SWNTs as an n-type thermoelectric material.

Results and Discussion

Encapsulation of cobaltocene in SWNTs. The $CoCp_2$@SWNTs were synthesized according to a method previously reported[26], and the high-resolution scanning transmission electron microscope (STEM) measurements of the sample were carried out. As shown in Figure S1, we observed aligned black dots that are attributed to the Co atoms of $CoCp_2$ that was encapsulated in the SWNTs. We measured the XPS narrow scans of Co_{2p} for the $CoCp_2$@SWNTs as well as the empty-SWNTs as a reference material. As shown in Fig. 2a, we clearly observed peaks assignable to the Co_{2p} in the $CoCp_2$@SWNTs (red line in Fig. 2a), while no such peak was recognized in the empty SWNTs. These results indicated not only the presence of $CoCp_2$, but also the encapsulation of $CoCp_2$ inside the SWNTs since $CoCp_2$ molecules easily sublimate even under atmospheric conditions and are rather difficult to detect under vacuum conditions used for this XPS measurement ($\sim 10^{-9}$ Pa)[28]. Interestingly, the peaks that appeared around 780 and 795 eV were assigned not to Co^{2+}, but Co^{3+}, due to the electron transfer from the $CoCp_2$ to the SWNTs. In addition, the shake-up satellites[28] observed at 785.5 eV and 790.3 eV due to Co^{2+} are significantly reduced in intensity, which indicates a change from neutral $CoCp_2$ to $CoCp_2^+$ via the charge transfer to the nanotubes. Indeed, the comparison of the C_{1s} photoemission spectra between the SWNTs and $CoCp_2$@SWNTs (Fig. 2b) revealed a change in symmetry at around 285 eV, and a decrease in the shake-up peaks at around 291 eV (indicated by the arrow) due to the electronic interaction between the SWNTs and encapsulated metallocene[29]. From the elemental analysis based on the XPS data, it was calculated that the $CoCp_2$@SWNTs contained 4.76 wt% of cobalt and more than 80% of the interior spaces were occupied by the $CoCp_2$ assuming that the molecular c-axis is perpendicular to the tubular axis and the intermolecular distance between the $CoCp_2$ molecule is 0.793 nm[30] as already reported.

In the TGA measurements under flowing air, we recognized an abrupt drop starting at around 570 K (red line in Fig. 2c) for the $CoCp_2$@SWNTs, which was much lower than that of the empty SWNTs (870 K, black line in Fig 2c). This significant difference is due to the catalytic effect of the Co metal[31]. The observed break temperature appeared at $\sim$570 K for the $CoCp_2$@SWNTs was clearly higher than the weight loss temperature of $CoCp_2$ (450 K, black dotted line in Fig. 2c) probably due to the electrostatic interaction between the SWNTs and $CoCp_2$. Based on the amount (14.5 wt%) of the residual black powder obtained after the TGA measurements that is assignable to Co_3O_4 from the Raman spectrum[32] (see Supplementary, Fig. S2), the amount of Co was estimated to be 5.9 wt%, which is close to the content (4.76 wt%) obtained by the XPS analysis.

Fig. 2d shows a comparison of the Raman spectra between the $CoCp_2$@SWNTs (red line) and SWNTs (black line), for which both samples had G/D band intensity ratios between the D band at $\sim$1350 cm^{-1} and G band at $\sim$1590 cm^{-1} that were almost identical, which guarantees that no structural defect was introduced upon encapsulation of the $CoCp_2$ since the G/D ratios reflect the formation of defects on the SWNTs. On the other hand, the normalized Raman spectra in the Radial Breathing Mode (RBM) region (red line in Fig. 2e) exhibited clear peak shifts and a decrease in the peak intensity due to the doping to the SWNTs with $CoCp_2$[17].

Furthermore, a comparison of the absorption spectra of the $CoCp_2$@SWNT and SWNT solution in D_2O with sodium dodecylbenzenesulfonate revealed that characteristic absorption peaks of both metallic and semiconducting SWNTs appeared around 600–800 and 900–1300 nm, respectively, red-shifted by $\sim$30 meV (Fig. 2f). The result suggested an n-type doping on the tubes by $CoCp_2$, which agreed with the previous report[26].

Thermoelectric property of $CoCp_2$@SWNT film. One of the advantages of the SWNTs is the formation of tough, but flexible film due to the entanglement of the fibrous SWNTs by facile filtration of the SWNT dispersions. In this study, two types of freestanding films of the $CoCp_2$@SWNTs (Fig. 3a) and the empty-SWNTs were fabricated. The SEM image of a $CoCp_2$@SWNT film (Fig. 3b) shows entanglement of the fibrous SWNTs and the length and diameter of the $CoCp_2$@SWNT bundles were $>$ 5 μm and 10–200 nm, respectively. The free-standing $CoCp_2$@SWNT film enabled to bent to a 3.5 mm-radius over 1,000 times-bending test without any change in the surface resistance (Fig. 3c), indicating high flexibility due to the entangled network structures as shown in Fig. 3b. These films were used to measure the electrical conductivities and Seebeck coefficients at different temperatures, and the results are shown in Fig. 3d and 3e, respectively. Of interest, the electrical conductivity of the $CoCp_2$@SWNT film increased by one order of magnitude (43,200 S m^{-1} at 320 K) compared to that (4,450 S m^{-1}) of the

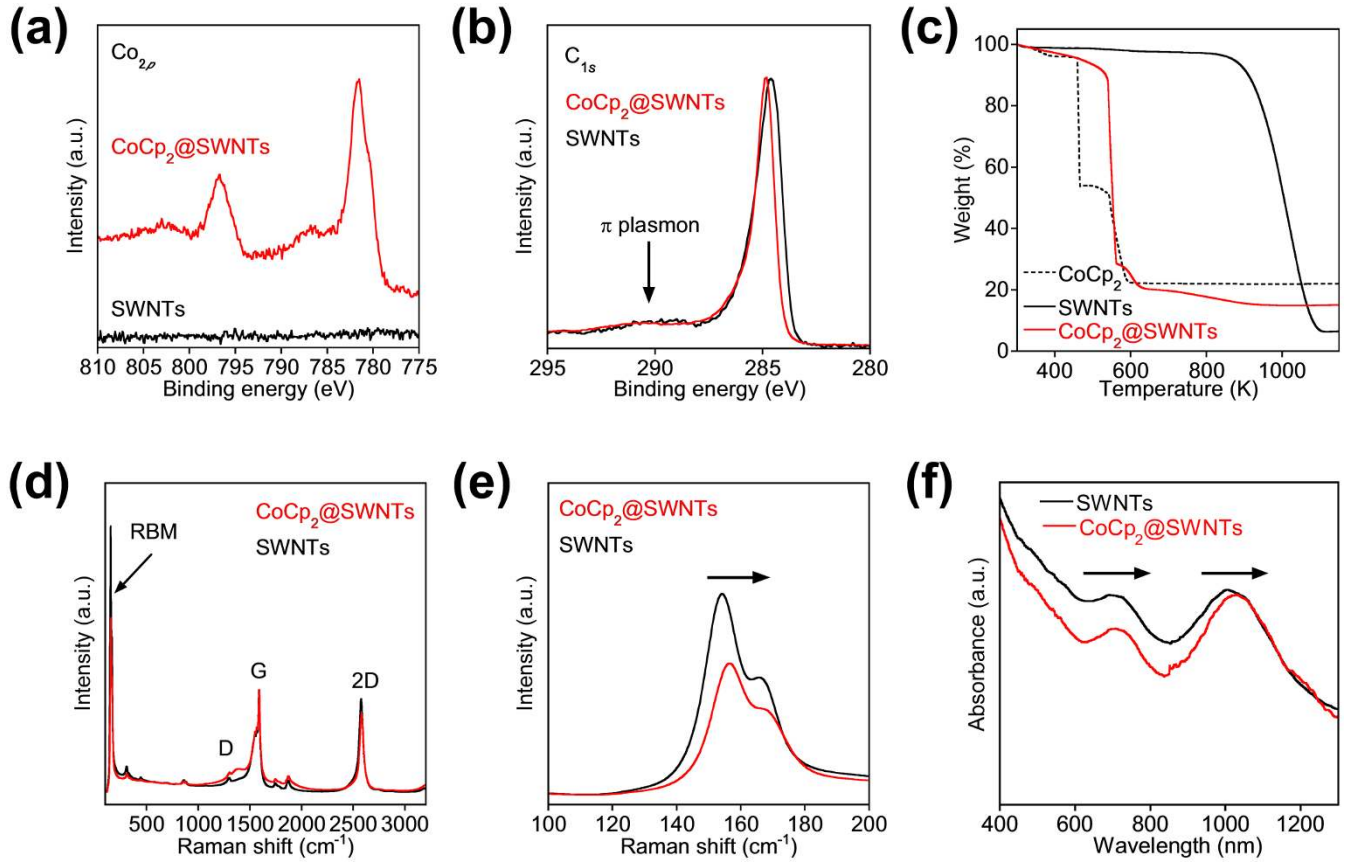

Figure 2 | XPS, TGA, Raman and absorption spectra of the $CoCp_2$@SWNTs. (a,b) XPS narrow scans of (a) Co_{2p} and (b) C_{1s} for the $CoCp_2$@SWNTs (red line) and SWNTs (black line). Shake-up peak is indicated by the arrow. (c) TGA curves of $CoCp_2$@SWNTs (red solid line), SWNTs (black solid line) and $CoCp_2$ (black dotted line) under flowing air (200 mL min^{-1}). (d,e) Raman spectra of the $CoCp_2$@SWNTs (red line) and empty SWNTs (black line) at (c) over a wide region and (d) the RBM region. The Raman intensity is normalized by the G band intensity. (f) Absorption spectra of $CoCp_2$@SWNT (red line) and SWNT (black line) dispersed in D_2O using sodium dodecylbenzenesulfonate (SDBS) as a dispersant.

empty SWNTs. The electrical conductivity of the $CoCp_2$@SWNTs film is higher than that of the SWNT film, which is explained by the increased carrier density, leading to an upshift of the Fermi level due to the charge transfer from the $CoCp_2$ to the nanotubes. From the XPS result shown in Figure 2a, the $CoCp_2$ was oxidized to $CoCp_2^+$, indicating the electron transfer from $CoCp_2$ to the tubes, and resulting in an increase in the carrier density of the nanotubes. Smalley et al.[18] also reported the increase of conductivity of the nanotubes by chemical doping using potassium and Br_2, resulting in increase of electrical conductivity due to an increase in carrier density. Furthermore, these values were almost constant in the temperature range of 310– 420 K. In order to explain the possible conduction mechanism of the $CoCp_2$@SWNT film, we analyzed the temperature dependent electrical conductivities based on the variable range hopping (VRH) models using the following equation (1),

$$\sigma(T) = \sigma_0 \exp[-(T_0/T)^{1/(d+1)}] \quad (1)$$

where $\sigma(T)$ and T are the electrical conductivity (S m^{-1}) and absolute temperature (K), respectively, and T_0 is a characteristic temperature used in the VRH model. d has a value of 1–3 (d = 1: Efros-Shklovskii (ES)-VRH, d = 2 or 3: Mott-VRH)[33]. Although the temperature-dependent electrical conductivities of the SWNT film were fitted well with the model similar with the previous study[33], for the $CoCp_2$@SWNT film, the temperature dependent electrical conductivities were not reproduced in the range of d =1–3 (see Supplementary, Fig. S3). The results suggested that the conduction mechanism of the $CoCp_2$@SWNT film differed from the VRH model. To reveal the conduction mechanism of the $CoCp_2$@SWNT film, further experiments such as magneto-resistance measurements are currently undergoing in our laboratory, and the results will be reported as a subsequent paper.

Most importantly, we found that the observed Seebeck coefficient of the $CoCp_2$@SWNT film showed a negative value (− 41.8 μV K^{-1} at 320 K), which corresponds to an n-type semiconductor, while that of the empty SWNT film was positive (45.3 μV K^{-1} at 320 K), which indicates the p-type nature. The conversion from the p-type semiconductor to the n-type semiconductor by encapsulation of $CoCp_2$ inside the nanotubes is derived from the change in charge carrier from holes to electrons due to the charge transfer from $CoCp_2$ to the nanotube, as indicated from the XPS data shown in Figure 2a. Kawai et al.[8] reported the relationship between the highest-occupied molecular orbital (HOMO) of dopants and the sign (i.e. positive/negative) of the Seebeck coefficient of the doped SWNT films. They reported that the dopants with HOMO above roughly 5.6 eV vs. vacuum altered the charge carrier of the carbon nanotubes from holes to electrons. The ionization energy of $CoCp_2$ (solid state) was reported to be ~4.0 eV vs. vacuum[34]. This indicates that it has sufficient electronic potential to reduce the SWNTs, which have an estimated reduction potential of the used SWNTs is ~4.2 V vs. vacuum[35]. This indicates that charge transfer from $CoCp_2$ to the nanotubes can occur, leading to the n-type semiconducting nature. Furthermore, based on the DFT calculations for the encapsulation of $CoCp_2$ inside the SWNTs, Green et al.[36] reported that the singly occupied molecular orbital (SOMO) of $CoCp_2$ is higher than the conduction band of the (n,0)SWNT (n = 13–18). Thus, the charge transfer can proceed from $CoCp_2$ to the SWNTs and the $CoCp_2$@SWNTs shows n-type semiconducting behaviour. These values

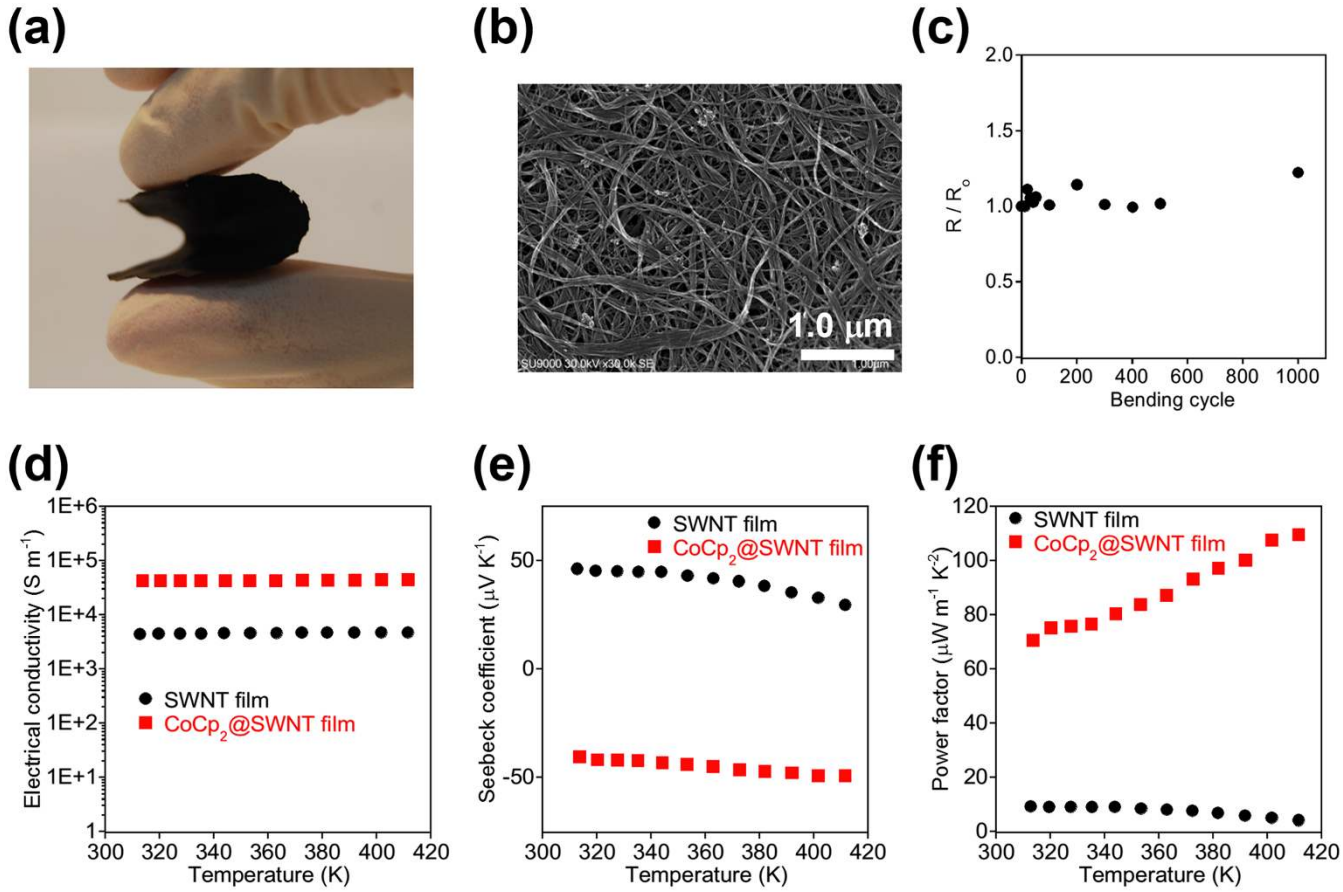

Figure 3 | Micrographs, mechanical, electrical and thermoelectric properties of the $CoCp_2$@SWNT film. (a) Photograph and (b) SEM image of a $CoCp_2$@SWNT film. Scale bar in Figure 3b, 1.0 μm. (c) Plots of normalized sheet resistance of $CoCp_2$@SWNT films as a function of bending cycles. Bending radius = 3.5 mm, R_o = initial resistivity, R = resistivity after given bending cycles. (d–f) Temperature dependence of (d) electrical conductivity, (e) Seebeck coefficient and (f) power factor of the $CoCp_2$@SWNT film (red squares) and empty SWNT film (black circles).

allowed us to calculate the power factor (W m^{-1} K^{-2}) using the following equation (2),

$$\text{Power factor} = S^2\sigma \tag{2}$$

where S and σ are the Seebeck coefficient (V K^{-1}) and electric conductivity (S m^{-1}), respectively. The power factor of the $CoCp_2$@SWNT film (75.4 μW m^{-1} K^{-2} at 320 K) is much larger than that of the SWNT film due to its higher electrical conductivity than that of the empty SWNT film (Fig. 3f), and the value was larger than any other reported n-type SWNT-based materials as shown in Table 1. Generally, the electrical conductivity and Seebeck coefficient show a trade-off nature[5–7]. However, in our $CoCp_2$@SWNT film, the high electrical conductivity is compatible to a large Seebeck coefficient compared with the other n-type SWNT films (Table 1). We assumed that the doping of $CoCp_2$ inside the SWNTs increased the charge carrier density and also modulated the electronic density of state of the SWNTs as well, as supported by our Raman and absorption results (Fig. 2e and Fig. 2f) as well as suggested by a previous experimental report[26] and theoretical studies[30,37–39]. Such a modulation provides a remarkably large power factor for the $CoCp_2$@SWNTs. On the other hand, the film prepared from the simple mixture of the SWNTs and $CoCp_2$ ($CoCp_2$/SWNT film) provided a positive Seebeck coefficient comparable with that of the SWNT film (for details, see Methods and Supplementary, Table S1) due to the removal of $CoCp_2$ from the film during the filtration. Such obtained results indicated a higher doping stability of the encapsulated $CoCp_2$ in the SWNTs than that of the $CoCp_2$/SWNT film.

To evaluate the thermoelectric figure of merit (ZT) of the SWNT film and $CoCp_2$@SWNT film, we determined the thermal conductivity (κ) using the following equation (3),

$$\kappa = C_p\alpha\rho \tag{3}$$

where C_p, α, and ρ are the specific heat capacity, thermal diffusivity, and density, respectively, and these numerical values are listed in Table S2. Interestingly, both films were found to possess much lower κ values (0.12 and 0.15 W m^{-1} K^{-1} for the SWNT film and $CoCp_2$@SWNT film, respectively) than the reported value of an individual SWNT (3500 W m^{-1} K^{-1})[40]. Instead, the obtained value was comparable to the reported random network SWNT films (0.1–0.2 W m^{-1} K^{-1})[8,41]. Such a low thermal conductivity would be derived from the huge interfacial thermal resistance (phonon-phonon Umklapp scattering)[42] and their low density of the films (0.6–0.8 g cm^{-3}, see Fig. 3b). Based on the result, we determined the ZT values using the following equation (4),

$$ZT = S^2\sigma T/\kappa \tag{4}$$

where S, σ, and T are the Seebeck coefficient (V K^{-1}), electric conductivity (S m^{-1}), and absolute temperature (K), respectively. The ZT value of the $CoCp_2$@SWNT film (0.157 at 320 K) was much higher than that of the SWNT film (0.025) due to its higher electrical conductivity than that of the SWNT film (Fig. 3e). Notably, the value was almost two times higher than that of the reported n-type CNT-based materials and the highest among the reported n-type organic thermoelectric materials (see Supplementary, Table S3)[7].

Table 1 | Electrical conductivity, Seebeck coefficient and power factor of the SWNT composites prepared in this study as well as the data taken from previous studies

Sample (film state)	Electrical conductivity [S m^{-1}]	Seebeck coefficient [μV K^{-1}]	Power factor [μW m^{-1} K^{-2}]	Year [Reference]
$CoCp_2$@SWNTs	43,000	−40.4	70.7	This study
SWNT/PEI[a]/PVDF[b]	-	−46	-	2014[24]
SWNT/dppp[c]	12,400	−52	25	2013[8]
SWNT/PEI/PVA[d]	-	−32	0.01	2013[44]
SWNT/PEI/$NaBH_4$[e]	6,000	−80	-	2012[43]
SWNT/PVP[f]	-	−30	-	2012[46]
SWNT/PEI	-	−40	-	2012[46]
SWNT/PVDF	-	−5	-	2012[47]

[a]PEI represents polyethyleneimine.
[b]PDVF represents polyvinylidene difluoride.
[c]dppp represents 1,3-bis(diphynyl phosphino)propane.
[d]PVA represents polyvinyl alcohol.
[e]$NaBH_4$ represents sodium borohydride.
[f]PVP represents polyvinylpyrroridone.

The SWNT film doped with cobaltocene as an n-type dopant is a very promising candidate for the next-generation thermoelectric materials due to its high electrical conductivity and the low thermal conductivity.

Thermoelectric device consisted of $CoCp_2$@SWNT and empty SWNT film. We then fabricated a typical π-shaped thermoelectric device[5–7] that is composed of films of the $CoCp_2$@SWNTs and empty-SWNTs as the n-type and p-type semiconducting materials, respectively, in which the two films are electrically connected by a thin Ni plate (Fig. 4a and 4b). It is important to note that the films have no protective coating, typically provided for such devices[8,43]. In Fig. 4c, the voltage generated upon heating of one ends of the films is plotted as the function of a temperature gradient between the two ends of the films. The thermoelectric power of the device was found to linearly increase with the temperature increasing gradient and reached 0.67 mV at a temperature gradient of 10 K, which well agrees with the calculated value (0.70 mV) based on the Seebeck coefficients of the two films ($CoCp_2$@SWNTs: ~-40 μV K^{-1}, SWNTs: ~30 μV K^{-1}). The deviation obtained from the estimated values (black dotted line in Fig.4c) for a greater temperature gradient would be derived from thermally-excited electrons and the contact resistance. We recognized the good reversibility by decreasing the temperature gradient (ΔT = 9 K was applied after applying ΔT = 20 K in Fig. 4c). The obtained reversibility strongly indicates that the deviation is caused by neither the absorption of molecules, such as water nor the oxidation by air since the water adsorption or oxidation was difficult to occur at such a low temperature. C. Yu et al. reported SWNTs doped with PEI underwent a severe deterioration of their doping effect in air, and, in such a device, the film needed to be laminated by a polyester to prevent the O_2 reduction for a stable thermoelectric power generation[44]. In sharp contrast, our device exhibited a stable power generation close to the calculated value with a good reversibility without any lamination due to the air stability of the encapsulated SWNTs[17]. In addition to such air stability, flexibility, toughness, thermal stability and light-weight of the device based on the carbon nanotube are quite attractive for a wide range of applications.

Since the power factor of the SWNT film was relatively low (9.1 μW m^{-1} K^{-1} at 320 K) compared to the absolute value of the $CoCp_2$@SWNT film (75.4 μW m^{-1} K^{-1} at 320 K) due to its lower electric conductivity, the development of the SWNT film with a higher electric conductivity by doping with a p-dopant, such as tetracyano-*p*-quinodimethane, is expected to enhance the performance of the device. In addition, the TGA curves of the $CoCp_2$@SWNTs measured under flowing nitrogen show a high thermal stability up to 700 K (see Supplementary, Fig. S4).

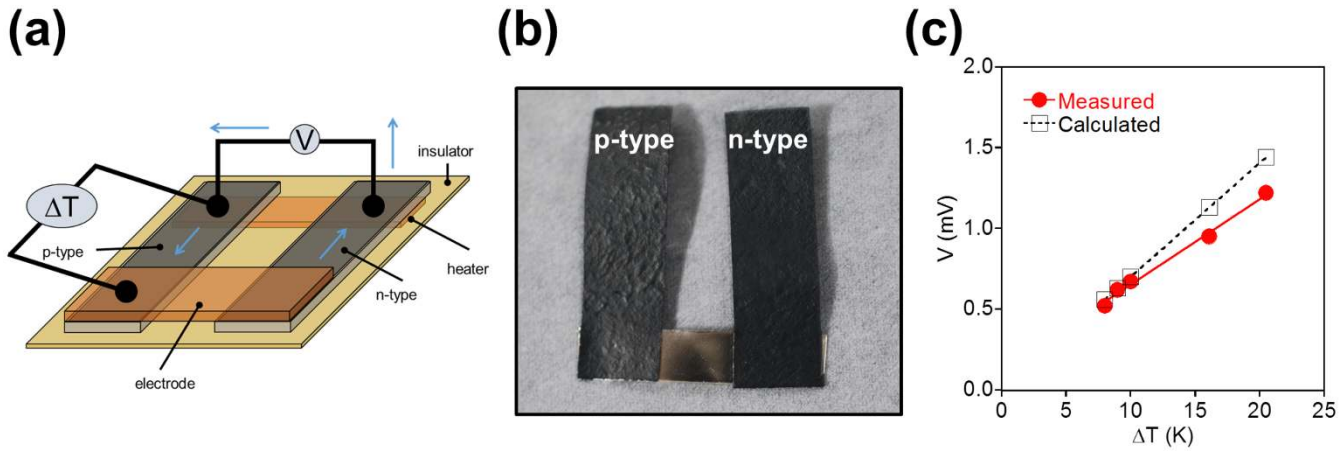

Figure 4 | The thermoelectric device based on the $CoCp_2$@SWNT and SWNT film. (a) Schematic illustration of the set-up for measuring the thermoelectric power generation. (b) Photograph of a thermoelectric device consisted of $CoCp_2$@SWNT film and SWNTs film as an n-type and p-type thermoelectric materials, respectively. (c) Measured (red circle) and calculated (black square) voltages generated from the thermoelectric device based on the $CoCp_2$@SWNTs and SWNTs as a function of the temperature gradient.

Conclusions

In conclusion, we synthesized cobaltocene-encapsulated SWNTs ($CoCp_2$@SWNTs) and found that the material showed a high electrical conductivity (43,200 S m^{-1}) as well as a negative Seebeck coefficient (−41.8 μV K^{-1}) at 320 K. Due to their high electrical conductivity, the power factor of the material was much larger (75.4 μW m^{-1} K^{-2}) than that of the films of empty-SWNTs (9.1 μW m^{-1} K^{-2}) at 320 K. The *ZT* value of the $CoCp_2$@SWNT film (0.157 at 320 K) was the highest among the reported n-type organic thermoelectric materials due to its high electrical conductivity and low thermal conductivity (0.15 W m^{-1} K^{-1}). The SWNT film doped with cobaltocene as an n-type dopant is a promising candidate for the next-generation thermoelectric materials due to the high electrical conductivity and low thermal conductivity. We demonstrated that the developed flexible thermoelectric device that consisted of a $CoCp_2$@SWNT film and empty SWNT film as the n- and p-doped semiconducting materials, respectively, generated voltages close to a calculated value with an excellent reversibility without any air-protective coating due to the characteristic air stability by the encapsulation. The device is quite attractive to collect a large amount of waste heat for electricity because the SWNT-based device is quite tough, flexible, and has a high thermal stability.

Methods

Materials. The SWNTs (Meijo-SO) with a ~1.4 nm diameter were purchased from Meijo Nanocarbon Co., Ltd., and purified according to a previous method[45]. Acetone, deuterium oxide (D_2O, 99.9%), ethanol, hydrochloric acid (12 M), hydrogen peroxide, *N*-methylpyrrolidone (NMP), sodium dodecylbenzenesulfonate (SDBS) and toluene were purchased from Wako Pure Chemical Industries, Ltd., and used as received. $CoCp_2$ was purchased from Aldrich and used as received.

Fabrication of a $CoCp_2$@SWNT film. $CoCp_2$ was encapsulated in the SWNTs in a manner similar to that previously reported using HiPco SWNTs[26]. The $CoCp_2$@SWNTs (15 mg) were dispersed in NMP (150 mL) using a bath-type sonicator (Branson 5010) for 1 h, then the dispersion was filtered through a 200-nm PTFE membrane. The obtained filter cake was washed with NMP and methanol, followed by drying at 353 K for 12 h under vacuum.

Fabrication of $CoCp_2$/SWNT film for comparison. SWNTs (15 mg) was dispersed in NMP (150 mL) containing $CoCp_2$ (5 mg) by a bath-type sonicator (Brinson 5010) for 1 h, then filtered with a 200-nm PTFE membrane filter. The obtained filter cake was wash with NMP and methanol, then dried at 353 K for 12 h under vacuum.

Preparation of $CoCp_2$@SWNT solution. The $CoCp_2$@SWNTs (1 mg) in a 1wt% SDBS solution in D_2O (10 mL) was sonicated for 1 h, and then ultra-centrifuged at 150,000 *g* for 3 h at 298 K. The top-80% of the supernatant was collected and used for this study. SWNT solution was prepared in the similar manner.

Fabrication of thermoelectric device. Each film of $CoCp_2$@SWNTs and empty-SWNTs was cut by ~15 × 4 mm, which were electrically connected to a Ni thin film (50 μm, Nilaco Co., Ltd.) using an Ag past (D-550, Fujikura Kasei Co., Ltd.).

Measurements. Raman spectroscopy was carried out using a Raman RXN Systems (Kaiser, excitation, 785 nm) at room temperature. X-ray photoelectron spectroscopy (XPS) was measured at room temperature using an AXIS-ULTRA (Shimadzu), in which indium was used as the substrate. Vis-NIR absorption spectrum was measured using a spectrophotometer (V-670, JASCO). Ultracentrifugation was carried out using a centrifugator (CS100GXL, Hitachi Koki). The thermogravimetric analysis (TGA) was carried out using an EXSTAR TG/DTA 6300 (SII Nanotechnology) at the heating rate of 10 K min^{-1} under flowing air or nitrogen (200 mL min^{-1}). Scanning electron microscopy (SEM) and scanning transmission electron microscope (STEM) measurements were carried out using an SU-9000 (Hitachi High Technologies, 30 kV acceleration voltage). $CoCp_2$@SWNTs (0.1 mg) were dispersed in methanol (3.0 mL) using a sonicator (Branson 5010). The resulting dispersion was then cast on an STEM Cu grid, then dried under vacuum at 353 K for 12 h. Bending durability test (Bending radius = 3.5 mm) was carried out by measuring the surface resistance of the film after bending cycles using a standard four-point probe resistivity meter (Loresta GP, Mitsubishi Chemical Analytech Co., Ltd.). The electrical conductivity and Seebeck coefficient of the samples on PTFE membrane filters were evaluated using a ZEM-3M (Ulvac-Riko) under helium at a reduced pressure (~0.01 MPa) to suppress the effect of gas convection and air oxidation during the measurement after annealing. The typical sample dimensions were 15, 4, and 0.02–0.03 mm for the length, width, and thickness, respectively. The voltage generated from the thermoelectric device was recorded using a digital multitester. Differential scanning calorimetry (DSC) was carried out using an EXSTAR DSC 6200 (SII Nanotechnology) at the heating rate of 10 K min^{-1} under flowing nitrogen (100 mL min^{-1}). Specific heat capacity (C_p) calibration was performed using a certified sapphire crystal (Al_2O_3). The thermal diffusivity was evaluated using a mobile-1 (ai-Phase Co., Ltd.). The density was determined from the weight and volume of the films.

1. Hochbaum, A. I. *et al.* Enhanced thermoelectric performance of rough silicon nanowires. *Nature* **451**, 163–167 (2008).
2. Zebarjadi, M., Esfarjani, K., Dresselhaus, M. S., Ren, Z. F. & Chen, G. Perspectives on thermoelectrics: from fundamentals to device applications. *Energy Environ. Sci.* **5**, 5147–5162 (2012).
3. Vineis, C. J., Shakouri, A., Majumdar, A. & Kanatzidis, M. G. Nanostructured Thermoelectrics: Big Efficiency Gains from Small Features. *Adv. Mater.* **22**, 3970–3980 (2010).
4. Sootsman, J. R., Chung, D. Y. & Kanatzidis, M. G. New and Old Concepts in Thermoelectric Materials. *Angew. Chem. Int. Ed.* **48**, 8616–8639 (2009).
5. Dubey, N. & Leclerc, M. Conducting Polymers: Efficient Thermoelectric Materials. *J. Polym. Sci. Part B* **49**, 467–475 (2011).
6. Poehler, T. O. & Katz, H. E. Prospects for polymer-based thermoelectrics: state of the art and theoretical analysis. *Energy Environ. Sci.* **5**, 8110–8115 (2012).
7. Zhang, Q., Sun, Y., Xu, W. & Zhu, D. Organic Thermoelectric Materials: Emerging Green Energy Materials Converting Heat to Electricity Directly and Efficiently. *Adv. Mater.* **26**, 6829–6851 (2014).
8. Nonoguchi, Y. *et al.* Systematic Conversion of Single Walled Carbon Nanotubes into n-type Thermoelectric Materials by Molecular Dopants. *Sci. Rep.* **3**, Artn 3344 (2013).
9. Suemori, K., Hoshino, S. & Kamata, T. Flexible and lightweight thermoelectric generators composed of carbon nanotube-polystyrene composites printed on film substrate. *Appl. Phys. Lett.* **103**, 153902 (2013).
10. Meng, C. Z., Liu, C. H. & Fan, S. S. A Promising Approach to Enhanced Thermoelectric Properties Using Carbon Nanotube Networks. *Adv. Mater.* **22**, 535–539 (2010).
11. Kim, D., Kim, Y., Choi, K., Grunlan, J. C. & Yu, C. H. Improved Thermoelectric Behavior of Nanotube-Filled Polymer Composites with Poly(3,4-ethylenedioxythiophene) Poly(styrenesulfonate). *ACS Nano* **4**, 513–523 (2010).
12. Moriarty, G. P. *et al.* Thermoelectric behavior of organic thin film nanocomposites. *J. Polym. Sci. Part B* **51**, 119–123 (2013).
13. Bounioux, C. *et al.* Thermoelectric composites of poly(3-hexylthiophene) and carbon nanotubes with a large power factor. *Energy Environ. Sci.* **6**, 918–925 (2013).
14. Nakai, Y. *et al.* Giant Seebeck coefficient in semiconducting single-wall carbon nanotube film. *Appl. Phys. Express* **7**, 025103 (2014).
15. Sun, Y. M. *et al.* Organic Thermoelectric Materials and Devices Based on p- and n-Type Poly(metal 1,1,2,2-ethenetetrathiolate)s. *Adv. Mater.* **24**, 932–937 (2012).
16. deLeeuw, D. M., Simenon, M. M. J., Brown, A. R. & Einerhand, R. E. F. Stability of n-type doped conducting polymers and consequences for polymeric microelectronic devices. *Synth. Met.* **87**, 53–59 (1997).
17. Takenobu, T. *et al.* Stable and controlled amphoteric doping by encapsulation of organic molecules inside carbon nanotubes. *Nat. Mater.* **2**, 683–688 (2003).
18. Lee, R. S., Kim, H. J., Fischer, J. E., Thess, A. & Smalley, R. E. Conductivity enhancement in single-walled carbon nanotube bundles doped with K and Br. *Nature* **388**, 255–257 (1997).
19. Kim, S. M. *et al.* Reduction-Controlled Viologen in Bisolvent as an Environmentally Stable n-Type Dopant for Carbon Nanotubes. *J. Am. Chem. Soc.* **131**, 327–331 (2009).
20. Klinke, C., Chen, J., Afzali, A. & Avouris, P. Charge transfer induced polarity switching in carbon nanotube transistors. *Nano Lett.* **5**, 555–558 (2005).
21. Kang, B. R. *et al.* Restorable Type Conversion of Carbon Nanotube Transistor Using Pyrolytically Controlled Antioxidizing Photosynthesis Coenzyme. *Adv. Funct. Mater.* **19**, 2553–2559 (2009).
22. Wang, H. L. *et al.* Tuning the threshold voltage of carbon nanotube transistors by n-type molecular doping for robust and flexible complementary circuits. *Proc. Natl. Acad. Sci. U. S. A.* **111**, 4776–4781 (2014).
23. Shimizu, R., Matsuzaki, S., Yanagi, K. & Takenobu, T. Optical Signature of Charge Transfer in n-Type Carbon Nanotube Transistors Doped with Printable Organic Molecules. *Appl. Phys. Express* **5**, 125102 (2012).
24. Hewitt, C. A., Montgomery, D. S., Barbalace, R. L., Carlson, R. D. & Carroll, D. L. Improved thermoelectric power output from multilayered polyethylenimine doped carbon nanotube based organic composites. *J. Appl. Phys.* **115**, 184502 (2014).
25. Czerw, R. *et al.* Identification of electron donor states in N-doped carbon nanotubes. *Nano Lett.* **1**, 457–460 (2001).
26. Li, L. J., Khlobystov, A. N., Wiltshire, J. G., Briggs, G. A. D. & Nicholas, R. J. Diameter-selective encapsulation of metallocenes in single-walled carbon nanotubes. *Nat. Mater.* **4**, 481–485 (2005).
27. Li, X. K. *et al.* Controlled Doping of Carbon Nanotubes with Metallocenes for Application in Hybrid Carbon Nanotube/Si Solar Cells. *Nano Lett.* **14**, 3388–3394 (2014).
28. Henrion, O. & Jaegermann, W. Surface redox reactions of cobaltocene adsorbed onto pyrolytic graphite (HOPG). *Surf. Sci.* **387**, L1073–L1078 (1997).
29. Shiozawa, H. *et al.* Fine tuning the charge transfer in carbon nanotubes via the interconversion of encapsulated molecules. *Phys. Rev. B* **77**, 153402 (2008).

30. Garcia-Suarez, V. M., Ferrer, J. & Lambert, C. J. Tuning the electrical conductivity of nanotube-encapsulated metallocene wires. *Phys. Rev. Lett.* **96**, 106804 (2006).
31. Aksel, S. & Eder, D. Catalytic effect of metal oxides on the oxidation resistance in carbon nanotube-inorganic hybrids. *J. Mater. Chem.* **20**, 9149–9154 (2010).
32. Tang, C. W., Wang, C. B. & Chien, S. H. Characterization of cobalt oxides studied by FT-IR, Raman, TPR and TG-MS. *Thermochim. Acta* **473**, 68–73 (2008).
33. Yanagi, K. *et al*. Transport Mechanisms in Metallic and Semiconducting Single-Wall Carbon Nanotube Networks. *ACS Nano* **4**, 4027–4032 (2010).
34. Chan, C. K. *et al*. N-type doping of an electron-transport material by controlled gas-phase incorporation of cobaltocene. *Chem. Phys. Lett.* **431**, 67–71 (2006).
35. Hirana, Y. *et al*. Empirical Prediction of Electronic Potentials of Single-Walled Carbon Nanotubes With a Specific Chirality (n,m). *Sci. Rep.* **3**, Artn 2959 (2013).
36. Sceats, E. L. & Green, J. C. Charge transfer composites of bis(cyclopentadienyl) and bis(benzene) transition metal complexes encapsulated in single-walled carbon nanotubes. *Phys. Rev. B* **75**, Artn 245441 (2007).
37. Cao, F. L., Ren, W., Xu, X. F., Tong, Y. X. & Zhao, C. Y. The structural, energetic and electronic properties of doped carbon nanotubes by encapsulation of MCp2 (M = Fe, Co, Ni): A theoretical investigation. *Chem. Phys. Lett.* **512**, 81–86 (2011).
38. Sceats, E. L. & Green, J. C. Noncovalent interactions between organometallic metallocene complexes and single-walled carbon nanotubes. *J. Chem. Phys.* **125**, 154704 (2006).
39. Lu, J. *et al*. Amphoteric and controllable doping of carbon nanotubes by encapsulation of organic and organometallic molecules. *Phys. Rev. Lett.* **93**, 116804 (2004).
40. Pop, E., Mann, D., Wang, Q., Goodson, K. & Dai, H. Thermal conductance of an individual single-wall carbon nanotube above room temperature. *Nano Lett* **6**, 96–100 (2006).
41. Prasher, R. S. *et al*. Turning Carbon Nanotubes from Exceptional Heat Conductors into Insulators. *Phys. Rev. Lett.* **102**, 105901 (2009).
42. Zhong, H. L. & Lukes, J. R. Interfacial thermal resistance between carbon nanotubes: Molecular dynamics simulations and analytical thermal modeling. *Phys. Rev. B* **74**, 125403 (2006).
43. Yu, C. H., Murali, A., Choi, K. W. & Ryu, Y. Air-stable fabric thermoelectric modules made of N- and P-type carbon nanotubes. *Energy Environ. Sci.* **5**, 9481–9486 (2012).
44. Piao, M. *et al*. Increasing the thermoelectric power generated by composite films using chemically functionalized single-walled carbon nanotubes. *Carbon* **62**, 430–437 (2013).
45. Kataura, H. *et al*. Optical properties of fullerene and non-fullerene peapods. *Appl. Phys. A* **74**, 349–354 (2002).
46. Piao, M. X., Alam, M. R., Kim, G., Dettlaff-Weglikowska, U. & Roth, S. Effect of chemical treatment on the thermoelectric properties of single walled carbon nanotube networks. *Phys. Status Solidi B* **249**, 2353–2356 (2012).
47. Hewitt, C. A. *et al*. Multilayered Carbon Nanotube/Polymer Composite Based Thermoelectric Fabrics. *Nano Lett.* **12**, 1307–1310 (2012).

Acknowledgments

This work was supported in part by the Low-Carbon Research Network (LCnet) and the Nanotechnology Platform Project (Molecules and Materials Synthesis) of the Ministry of Education, Culture, Sports, Science and Technology (MEXT), Japan. Part of this research was supported by the Adaptable and Seamless Technology Transfer Program through Target-driven R&D, JST (AS242Z00200L) and the Advanced Low Carbon Technology Research and Development Program (ALCA). We also acknowledge the support by JST through its "Center of Innovation Science and Technology based Radical Innovation and Entrepreneurship Program (COI Program).

Author contributions

Ts.F. and N.N proposed and supervised the project. Ta.F designed experiments and analyzed the data. Ta.F, Ts.F. and N.N wrote the paper. All authors reviewed the manuscript.

Additional information

Supplementary information accompanies this paper at http://www.nature.com/scientificreports

Competing financial interests: The authors declare no competing financial interests.

How to cite this article: Fukumaru, T., Fujigaya, T. & Nakashima, N. Development of n-type cobaltocene-encapsulated carbon nanotubes with remarkable thermoelectric property. *Sci. Rep.* **5**, 7951; DOI:10.1038/srep07951 (2015).